Environmental Toxicology

Modulatory Effects of Mercury (II) Chloride (HgCl$_2$) on Chicken Macrophage and B-Lymphocyte Cell Lines with Viral-Like Challenges In Vitro

Biyao Han,* Diego García-Mendoza, Hans van den Berg, and Nico W. van den Brink

Division of Toxicology, Wageningen University and Research, Wageningen, The Netherlands

Abstract: Mercury (Hg) is a toxic trace metal ubiquitously distributed in the environment. Inorganic mercury (as HgCl$_2$) can cause immunotoxicity in birds, but the mechanisms of action are still not fully resolved, especially with respect to responses to viral infections. To investigate the potential immunomodulatory effects of Hg^{2+} on specific cell types of the avian immune system, chicken macrophage (HD-11) and B-lymphocyte (DT40) cell lines were applied as in vitro models for the innate and adaptive immune systems, respectively. The cells were stimulated with synthetic double-stranded RNA, which can be recognized by toll-like receptor-3 to mimic a viral infection. The Hg^{2+} showed concentration-dependent cytotoxicity in both cell lines, with similar median effect concentrations at 30 μM. The cytotoxicity of Hg^{2+} was closely related to glutathione (GSH) depletion and reactive oxygen species induction, whereas the de novo synthesis of GSH acted as a primary protective strategy. Nitric oxide produced by activated macrophages was strongly inhibited by Hg^{2+}, and was also influenced by cellular GSH levels. Cell proliferation, gene expression of microRNA-155, and cellular IgM levels in B cells were decreased at noncytotoxic Hg^{2+} concentrations. The secretion of antiviral interferon-α was induced by Hg^{2+} in both cell lines. Overall, our results suggest that Hg^{2+} exposure can cause immunomodulatory effects in birds by disrupting immune cell proliferation and cytokine production, and might result in disorders of the avian immune system. *Environ Toxicol Chem* 2021;40:2813–2824. © 2021 The Authors. *Environmental Toxicology and Chemistry* published by Wiley Periodicals LLC on behalf of SETAC.

Keywords: Mercury (II) chloride; Mercury ion; Avian; Immunotoxicity; Macrophages; B-lymphocytes; Viral-like challenges

INTRODUCTION

Mercury (Hg) is one of the trace metals that ubiquitously occurs in the environment, and human activities, such as mining and industry, have considerably elevated its environmental levels and global distribution (Dorea & Donangelo, 2006; Beckers & Rinklebe, 2017). Like other nonessential trace metals, Hg is regarded as a priority environmental contaminant due to its potential for bioaccumulation and biomagnification, and also its high toxicity (Mann et al., 2011). The major species of Hg include elemental mercury (Hg(0)), inorganic mercury (predominantly divalent mercury, Hg(II)), and organic mercury (mainly methylmercury, MeHg).

Although MeHg is recognized as the most toxic form, Hg(II) is more commonly and abundantly found in the environment (Schlüter, 2000; Beckers & Rinklebe, 2017) and can also exert severe adverse effects on wild animals. Elevated Hg levels have been detected in wild birds, affecting multiple physiological parameters including immune functions (Thaxton & Parkhurst, 1973; Wolfe et al., 1998; Ackerman et al., 2016; Whitney & Cristol, 2018). For example, tree swallows in a Hg-contaminated area showed compromised immune competence, with weaker skin swelling responses to phytohemagglutinin challenge (Hawley et al., 2009). Elevated levels of internal Hg were associated with decreased macrophage phagocytosis in black-footed albatrosses (Finkelstein et al., 2007). The impact of Hg on the functioning of the immune system may result in higher risk of infections at individual levels and may cause prevalence of diseases (e.g., avian influenza) in the populations.

As just mentioned, for avian species, there are some in vivo and wildlife studies revealing the immune modulatory effects of Hg, but very limited knowledge on the cellular mechanisms and immune functional effects of Hg toxicity has

2814

Environmental Toxicology and Chemistry, 2021;40:2813–2824—B. Han et al.

been documented. More insights into the immunotoxicity of Hg were reported in studies using mammalian or human in vitro cell models (Loftenius et al., 1997; Silva et al., 2005; Das et al., 2008; Lehmann et al., 2011; Levin et al., 2020; Yang et al., 2020). Such in vitro studies can demonstrate the underlying mechanisms and can also reduce animal experiments. In vitro evidence has shown that the mechanisms of Hg-induced toxicity in immune cells are related to the induction of oxidative stress, the inhibition of nitric oxide, and the disturbance of cytokine profiles (Kim et al., 2002; Kim & Sharma, 2004; Guzzi & La Porta, 2008). However, this is based on mammalian models, whereas little is known about the cellular mechanisms of Hg-induced immunomodulatory effects in avian species.

To evaluate the effects of Hg exposure on avian immune functions, one should consider not only the baseline immunity but also the activated immunity, which is more relevant to vulnerability to diseases. Once infected by certain pathogens, avian immune cells recognize the pathogen-associated molecular patterns with specific receptors and trigger multiple defence strategies (Mogensen, 2009). For instance, toll-like receptor 3 (TLR3) can detect the double-stranded RNA (dsRNA) produced by most viruses during their replication (Sen & Sarkar, 2005). After immune activation, macrophages can produce nitric oxide and undergo oxidative burst to kill the pathogens (MacMicking et al., 1997), and B-lymphocytes can produce antibodies to neutralize the pathogens (Dörner & Radbruch, 2007). To mediate the immune responses and communicate with other cells, immune cells also produce cytokines with various functions, such as antiviral interferon-α and β (IFN-α and -β), interleukins ([ILs] e.g., pro-inflammatory IL-18) and chemokines (e.g., IL-8; Kaiser & Stäheli, 2013). Apart from cytokines, microRNAs (miRNAs) also play an important role in regulating the immune responses; miRNAs such as miR-155 and let-7 are involved in the inflammatory response, cytokine production, and lymphocyte maturation (Gottwein et al., 2007; Lu & Liston, 2009; Staedel & Darfeuille, 2013; Kumar et al., 2015; Alivernini et al., 2018). An adequate immune response requires an appropriate population of functional immune cells and proper levels of immune mediators (namely, cytokines and miRNAs) for communication and cooperation among different immune cells.

The aim of the present study was to investigate the modulatory effects and potential mechanisms of Hg^{2+} on the avian immune systems using chicken macrophage (HD-11) and B-lymphocyte (DT40) cell lines as in vitro models for the innate and adaptive immune systems, respectively, with and without a mimicked viral challenge with dsRNA. Both cell lines have been documented to express TLR3 and could be stimulated with dsRNA (Peroval et al., 2013; Quan et al., 2017). General toxicity (cytotoxicity, oxidative stress) and functional endpoints were quantified, including nitric oxide production by macrophages, cell proliferation, immune gene expression (receptors, cytokines, and miRNAs), and immune protein levels (cytokines and antibodies) as indicators for immunity after Hg^{2+} exposure and activation.

MATERIALS AND METHODS

Cell culture

The HD-11 chicken macrophage cell line was a kind gift from J. van Baal (Department of Animal Sciences, Wageningen University, The Netherlands) and was cultured in RPMI 1640 medium (Gibco) with 10% fetal bovine serum (FBS; Sigma-Aldrich) at 37 °C in a 5% CO_2 humidified air incubator. Every 2–3 days, HD-11 cells were subcultured by detaching the cells with 5 mM ethylenediaminetetraacetic acid (EDTA; Merck) and diluting the cell suspension with fresh culture medium. A washing step with phosphate-buffered saline (PBS; Gibco) was performed before seeding the cells to remove the EDTA.

The chicken B-lymphocyte cell line DT40 (ATCC® CRL2111™) was maintained in Dulbecco's modified Eagle medium (Gibco) containing 10% FBS, 10% tryptose phosphate broth (Sigma-Aldrich), 5% chicken serum (Sigma-Aldrich), and 0.05 mM 2-mercaptoethanol (Gibco) at 37 °C in a 5% CO_2 humidified air incubator. Cells were subcultured every 2–3 days by diluting the cell suspension with fresh culture medium.

Experimental setup

Effects of Hg^{2+} (as mercury (II) chloride $[HgCl_2]$) exposure on general cytotoxicity and immune functions were investigated in HD-11 chicken macrophages and DT40 chicken B-lymphocytes. Both cell lines are able to be activated with dsRNA via the TLR3 pathway (He et al., 2007; Keestra & van Putten, 2008; Zou et al., 2017; Ma et al., 2019). Therefore, we used a synthetic analog of dsRNA, polyinosinic–polycytidylic acid sodium salt (poly I:C; Alexopoulou et al., 2001; Matsumoto & Tsukasa, 2008), to induce viral-like challenges in all assays in the present study.

Metal ions including Hg^{2+} have a high affinity for thiol groups and can deplete the major intracellular antioxidant glutathione (GSH), resulting in oxidative stress and cytotoxicity (Hultberg et al., 2001; Nuran Ercal et al., 2005; Hossain et al., 2021). To reveal the possible underlying mechanism of Hg^{2+} toxicity related to GSH depletion, co-exposure with the γ-glutamylcysteine synthetase blocker L-buthionine-sulfoximine (BSO) was introduced to inhibit de novo GSH synthesis. The water-soluble tetrazolium-1 (WST-1) assay was used to determine the median effect concentration (EC50) values after 24-h exposure to Hg^{2+} in cells treated under different conditions, including immune activation with 25 µg/ml poly I:C (Sigma-Aldrich) and inhibition of the de novo GSH synthesis by 200 µM BSO (Sigma-Aldrich). These EC50 values served as the basis for defining the concentration ranges in follow-up assays. Changes in intracellular GSH and reactive oxygen species (ROS) levels due to Hg^{2+} exposure were investigated to elucidate their potential role in the mechanism(s) of Hg^{2+}-induced toxicity.

Afterward, effects of Hg^{2+} exposure on immune functions were assessed. Production of nitric oxide by HD-11 cells was quantified as a primary functional endpoint for macrophages. Cell proliferation was examined using both the WST-1 assay for metabolic activity (cell activity), and the bromodeoxyuridine (BrdU) assay for DNA synthesis (cell division) with extended

exposure time (48 h) in both cell lines. In addition, expression of immune function genes and miRNAs after Hg^{2+} exposure was profiled with quantitative reverse transcription polymerase chain reaction (RT-qPCR) at the transcription level. Finally, enzyme-linked immunosorbent assays (ELISAs) were employed to measure multiple immune functional protein levels, including the production of type I antiviral IFN-α in the supernatant of both cell lines, and immunoglobulin M (IgM) levels in both supernatant (for secreted IgM) and cell lysate (for cellular IgM) of DT40 B-lymphocytes. All the assays were performed in three independent experiments and carried out as described hereafter.

Exposure

For most of the assays, either HD-11 macrophages or DT40 B-cells were seeded at a density of 1×10^5 cells/well in a clear, flat-bottomed 96-well plate and incubated overnight before exposure. In proliferation assays, 1×10^4 cells/well were seeded, allowing a longer exposure time (48 h). For RT-qPCR, 1×10^6 cells/well were seeded in 12-well plates. A series of HgCl$_2$ (Sigma-Aldrich) stock solutions ranging from 0.2 to 2000 μM were prepared in sterile Milli-Q water and diluted 20 times in culture medium to the final exposure concentration, ranging from 0.01 to 100 μM. Then 5 mg/ml poly I:C stock solution was prepared in PBS and stored at –20 °C. To activate the cells, poly I:C (Sigma-Aldrich) stock solution was diluted 200 times in culture medium to a final concentration of 25 μg/ml in all assays. Also, to block de novo GSH synthesis via γ-glutamylcysteine synthetase, 200 μM (final concentration) of BSO was added to the culture medium of the cells in the cytotoxicity, GSH, ROS, and nitric oxide assays. Exposure to HgCl$_2$, poly I:C, and BSO started at the same time. Exposure time was 24 h for most assays, except for the proliferation assays, in which the exposure time was prolonged to 48 h.

General toxicity assays

Cytotoxicity assay. Cells were exposed to Hg^{2+} in four conditions, namely, with or without 200 μM BSO to block de novo GSH synthesis and with or without 25 μg/ml poly I:C activation. After 20 h of exposure, 10 μl (5% v/v) WST-1 reagent was added to each well of HD-11 or DT40 cells and incubated at 37 °C for 4 h before measuring absorbance at 440 nm and a reference wavelength at 620 nm with a SpectraMax M2 Microplate Reader (Molecular Devices). Cell viability was expressed as percentage of negative controls in the non-BSO, nonactivated treatment group (–BSO –poly I:C group). Concentrations of Hg^{2+} used in the later assays were based on the results obtained for Hg^{2+} in cell viability assays.

GSH assay. ThiolTracker™ Violet Glutathione Detection Reagent (Life Technologies) was used to measure the intracellular GSH levels after Hg^{2+} exposure. Briefly, after 20 h of exposure, cells were washed twice with Dulbecco's phosphate-buffered saline with calcium and magnesium (D-PBS C/M; Gibco). Cells were then labeled with 20 μM ThiolTracker Violet dye working solution for 30 min at 37 °C. After they were washed for another two times with D-PBS C/M,

cells were resuspended, and fluorescence was measured at ex/em 404/526 nm with the SpectraMax M2 Microplate Reader. The GSH levels were shown as percentages relative to the negative controls in the –BSO –poly I:C group.

ROS assay. The ROS levels inside the cells were measured with 2′,7′-dichlorofluorescin diacetate (DCFDA; Sigma-Aldrich) reagent after 24 h of Hg^{2+} exposure. Once diffused into the cell and de-esterified by cellular esterase, DCFDA is oxidized to highly fluorescent 2′,7′-dichlorofluorescin (DFC) by ROS (Rosenkranz et al., 1992). The exposure conditions were identical to those of the cytotoxicity and GSH assays (also with or without poly I:C and BSO). Cells were first exposed for 20 h and then labeled with 25 μM DCFDA for another 4 h before fluorescence measurement at ex/em 485/535 nm. Results are presented as ratios relative to the negative controls in the –BSO –poly I:C group.

Immune functional assays

Nitric oxide (Griess) assay. Nitric oxide produced by HD-11 macrophages under the same exposure conditions as the ones used in the cytotoxicity, GSH, and ROS assays was examined using the Griess assay (Sun et al., 2003). Briefly, after 24 h of exposure, 100 μl of exposed cell culture supernatant was transferred to a new 96-well plate. Then 50 μl of 1% sulfanilamide (Sigma-Aldrich) in 5% phosphoric acid (Merck) and 50 μl of 0.1% *N*-(1-naphthyl)ethylenediamine dihydrochloride (Sigma-Aldrich) solution were added to the supernatant successively with a 5-min interval. The plates were incubated for 5 min in the dark between the addition of the two solutions and before measuring absorbance at 540 nm with the SpectraMax M2 Microplate Reader. Nitric oxide production after treatment was calculated based on a calibration curve of NaNO$_2$ ranging from 1.56 to 100 μM.

Proliferation assays. Two endpoints, namely, cell activity and cell division, were tested to evaluate cell proliferation levels after 48 h of Hg^{2+} exposure. The WST-1 assay was performed as described previously in the *Cytotoxicity assay* section. The colorimetric BrdU assay (Roche) was applied according to the manufacturer's instructions. Briefly, during the last 4 h of exposure, newly synthesized DNA in the cells was labeled with BrdU. Floating DT40 cells were separated by centrifugation at 300 *g* for 10 min. Then both HD-11 and DT40 cells were fixed and incubated with anti-BrdU-POD antibody, which bound to the BrdU and reacted with the substrate. The reaction was terminated by adding stop solution after incubation with the substrate for 30 min at room temperature. Cell division (DNA synthesis) was quantified by absorbance at 450 nm with a reference at 690 nm and expressed as a percentage relative to the negative control in the nonactivated group (–poly I:C group).

Gene expression. Expression of nine chicken genes (six for messenger [m]RNA and three for miRNA), including a housekeeping gene (glyceraldehydes-3-phosphate dehydrogenase

2816

Environmental Toxicology and Chemistry, 2021;40:2813–2824—B. Han et al.

[GAPDH]), the genes for type I interferons (IFN-α, IFN-β), interleukins (IL-8, IL-18) and toll-like receptors recognizing viral pathogens (TLR7), reference miRNA (small nucleolar RNA, C/D box 68 [SNORD68]), and miRNAs involved in immune regulation (miR-155 and let7) were tested in both cell lines by RT-qPCR. All kits used were from Qiagen. Briefly, after 24 h of exposure, cells cultured in 12-well plates were lysed with QIAzol Lysis Reagent, and RNA was extracted using an miRNeasy Mini Kit. The quality and quantity of extracted RNA were checked by Nanodrop (ND-1000; Themoscientific). Then 300 ng total RNA was reverse-translated to cDNA using the miScript II RT Kit with miScript HiFlex Buffer to get complementary (c)DNA for both mRNA and miRNA. Then RT-qPCR was performed on a Rotor-Gene® 6000 cycler with either the QuantiNova SYBR® Green PCR Kit for mRNA or the miScript SYBR® Green PCR Kit for miRNA. Commercially available primer assays were used for immune functional genes, including QuantiTect® primer assays (Gg_GAPDH_1_SG, Gg_IFNA3_1_SG, Gg_IFNB_1_SG, Gg_IL8L2_1_SG, Gg_IL18_1_SG, and Gg_TLR7_1_SG) for mRNA expression and miRCURY LNA miRNA PCR Assay for miRNA primers (dre-miR-155, hsa-let-7a-5p, and SNORD68). The efficiency of qPCR amplification was checked for each primer using a 4-fold serial dilution standard curve prior to sample measurement.

Immune protein levels. Multiple immune functional proteins produced by the two cell lines, including IFN-α by both cell lines as well as IgM (both released and cellular) by DT40 B-lymphocytes, were quantified with commercially available sandwich ELISA kits. All the ELISA kits (chicken IFN-α and chicken IgM ELISA kits) were obtained from ELISAGenie. Assays were conducted according to the instructions provided by manufacturer for each kit.

Supernatant and cells were separated after exposure by centrifugation at 1000 *g* for 20 min at 4 °C. The IFN-α levels were measured in the supernatant samples from both HD-11 and DT40 cells, whereas the IgM levels were only analyzed in the supernatant of DT40 cells. Cellular IgM content was also determined in cell lysate prepared through three repeated freeze–thaw cycles after removal of the supernatant. Quantities of each immune protein (in pg/ml for IFN-α and ng/ml for IgM) were calculated by comparing absorbance at 450 nm with standard curves from each kit. Levels of IgM in cell lysate samples were expressed in ng/µg protein by normalizing with total protein content. Protein content was quantified with a Pierce™ BCA Protein Assay Kit (Thermo Fisher Scientific) according to the manufacturer's instruction.

Statistics

Statistical analyses and visualization of results were performed with GraphPad Prism 5. Concentration–response curves were fitted with nonlinear regression (variable slope, four parameters) to calculate EC50 values. One-way analysis of variance with Dunnett's post hoc test was conducted to compare treatment groups with Hg^{2+}-free controls. Gene expression levels were normalized against the housekeeping gene GAPDH (for mRNA) or SNORD68 (for miRNA) and shown as log2 fold changes in comparison with the negative control of nonactivated cells by the $-\Delta\Delta CT$ method (Schmittgen & Livak, 2008).

RESULTS

General toxicity

Cytotoxicity. Concentration–response curves for the effect of Hg^{2+} on both HD-11 and DT40 cells were obtained and showed similar EC50 values of approximately 30 µM irrespective of the poly I:C activation when the cells were not treated with BSO (Figure 1). When the de novo synthesis of GSH was blocked by cotreatment with BSO, Hg^{2+} showed much higher cytotoxicity in both cell lines. In HD-11 macrophages, the EC50 of Hg^{2+} for cells cotreated with BSO was 2.54 µM, and the EC50 for cells treated with both BSO and poly I:C was as low as 0.75 µM. A more potent effect of Hg^{2+} exposure was seen in BSO-treated DT40 B-lymphocytes, with EC50 values that were lower than 0.5 µM. An overview of all EC50 values is shown in Table 1. In HD-11 macrophages, poly I:C increased the cell metabolic activity by approximately 50%,
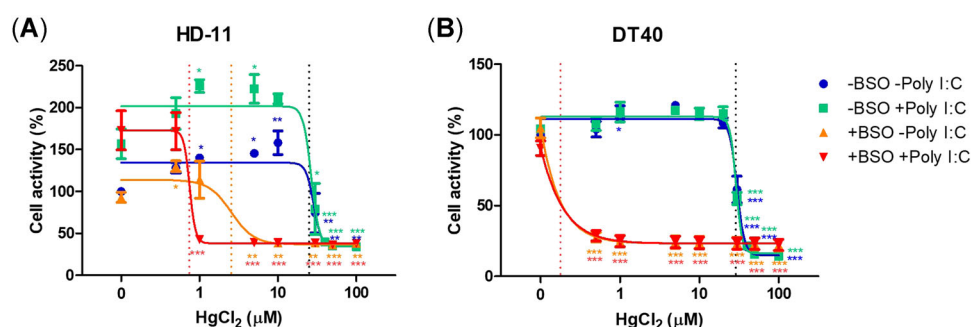

FIGURE 1: Cytotoxicity effects of mercury $(Hg)^{2+}$ on nonactivated and activated (25 µg/ml polyinosinic–polycytidylic acid sodium salt [poly I:C]) HD-11 (A) and DT40 (B) cells with or without glutathione synthesis inhibitor (200 µM L-buthionine-sulfoximine [BSO]) after 24-h exposure. Results are expressed as mean ± standard error of the mean (*n* = 3), relative to negative control in nonactivated cells for cell viability. Significant differences between treatments and Hg^{2+}-free controls were checked with one-way analysis of variance (*p < 0.05, **p < 0.01, ***p < 0.005). Vertical lines indicate the median effect concentrations (EC50s) for different treatment groups: red lines for the treatment groups with both BSO and poly I:C (+BSO +Poly I:C), orange lines for the treatment groups with BSO but without poly I:C (+BSO −Poly I:C), and black lines for the treatment groups without BSO because they showed similar EC50s.

TABLE 1: Overview of median effect concentration (95% confidence intervals) values of Hg^{2+} exposure for different endpoints

		−BSO −Poly I:C	−BSO +Poly I:C	+BSO −Poly I:C	+BSO +Poly I:C
Cytotoxicity	HD-11	29 µM (24.08–34.11)	27 µM (17.02–41.77)	2.54 µM (1.05–6.15)	0.75 µM (0.29–1.96)
	DT40	30 µM (28.28–31.35)	29 µM (27.76–30.37)	<0.5 µM n.a.	<0.5 µM n.a.
GSH	HD-11	16 µM (12.90–9.67)	15 µM (11.73–20.00)	2.28 µM (1.65–3.19)	0.82 µM (0.72 to 0.94)
	DT40	50~100 µM n.a.	50~100 µM n.a.	<0.5 µM n.a.	<0.5 µM n.a.
ROS	HD-11	6.51 µM (5.16–8.21)	6.56 µM (4.78–9.02)	0.54 µM (0.43–0.68)	0.79 µM (0.48–1.29)
Nitric oxide	HD-11	n.a.	3.85 µM (2.70–5.49)	n.a.	0.37 µM (0.17–0.78)
Proliferation: WST-1	HD-11	5.43 µM (3.74–7.87)	5.78 µM (3.94–8.47)	n.a.	n.a.
	DT40	5.60 µM (4.68–6.69)	4.28 µM (3.55–5.16)	n.a.	n.a.
Proliferation: BrdU	HD-11	6.32 µM (5.04–7.93)	5.31 µM (5.02–5.62)	n.a.	n.a.
	DT40	2.82 µM (1.40–5.70)	2.67 µM (1.09–6.54)	n.a.	n.a.
IFN-α	DT40	0.58 µM (0.10–3.24)	0.53 µM (0.35–0.79)	n.a.	n.a.

BSO = L-buthionine-sulfoximine; poly I:C = polyinosinic–polycytidylic acid sodium salt; GSH = glutathione; ROS = reactive oxygen species; WST-1 = water-soluble tetrazolium-1; BrdU = bromodeoxyuridine; IFN-α = interferon-α; n.a. = not applicable.

whereas no induction was seen in DT40 B-lymphocytes (Figure 1). In addition, noncytotoxic levels of Hg^{2+} exposure resulted in a significant increase of cell metabolic activity in cells not exposed to BSO, especially in HD-11 cells.

GSH and ROS. Different patterns of intracellular GSH depletion were demonstrated in HD-11 cells under different exposure conditions (Figure 2A). When the cell could still synthesize GSH (without BSO), a steep decrease in GSH levels was only found close to the EC50 of Hg^{2+} cytotoxicity, regardless of the activation. However, when the de novo synthesis of GSH was inhibited by BSO, GSH levels declined at much lower Hg^{2+} exposure concentrations, with an EC50 of 2.3 µM (with BSO but without poly I:C), which is approximately 5 times lower than the EC50 obtained without BSO (~15 µM). Cells cultured with both BSO and poly I:C were the most vulnerable, with an even lower EC50 of 0.82 µM Hg^{2+} and a significant decrease in their GSH level already at the lowest exposure concentration (0.5 µM). In HD-11 cells, the EC50 values for GSH depletion were in the same range as cytotoxicity for the individual treatment groups (shown as the vertical dashed lines in Figure 2A). As for DT40 cells, poly I:C did not affect the GSH changes, whereas BSO played a major role (Figure 2B). After blocking of the synthesis of GSH, GSH levels inside the cells sharply dropped to background

levels already at the lowest Hg^{2+} exposure concentration (0.5 µM). Nevertheless, GSH levels were not affected at noncytotoxic Hg concentrations in the absence of BSO in DT40 B-cells.

Similar to the results for GSH, patterns of ROS induction by Hg^{2+} exposure were influenced by the inhibition of de novo synthesis of GSH by BSO. In HD-11 cells, Hg^{2+} induced ROS up to approximately 6-fold under all four exposure conditions (Figure 3A). The EC50 values in cells co-exposed with BSO (without poly I:C 0.54 µM, with poly I:C 0.79 µM) were approximately 10 times lower than the EC50 values in cells that still could produce GSH (without poly I:C 6.51 µM, with poly I:C 6.56 µM). The poly I:C activation doubled the ROS levels in nonexposed HD-11 cells but did not affect the EC50 values of Hg^{2+} exposure. In DT40 cells, no significant induction of ROS was observed due to poly I:C activation, whereas ROS induction caused by Hg^{2+} exposure mainly occurred at cytotoxic concentrations above the EC50 values derived for cytotoxicity (shown as the vertical dashed lines in Figure 3).

Immune functional endpoints

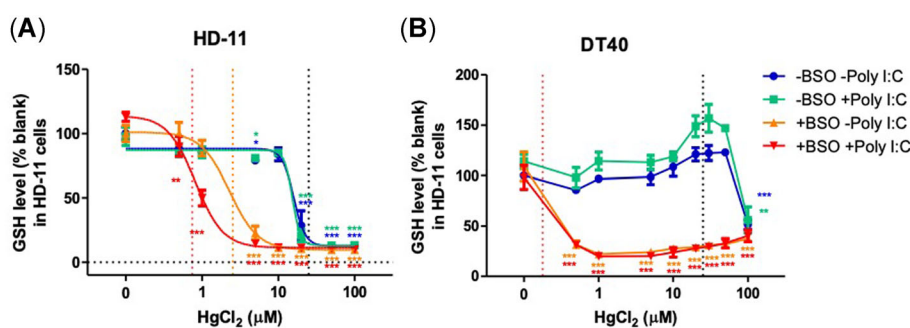*Nitric oxide.* Unlike the results in GSH and ROS, the patterns of nitric oxide production by HD-11 macrophages after Hg^{2+}

FIGURE 2: Intracellular glutathione (GSH) levels after 24-h exposure to mercury (Hg)$^{2+}$ in nonactivated and activated (25 µg/ml polyinosinic–polycytidylic acid sodium salt [poly I:C]) HD-11 (**A**) and DT40 (**B**) cells with or without GSH synthesis inhibitor (200 µM L-buthionine-sulfoximine [BSO]). Results are expressed as percentage (mean ± standard error of the mean, $n = 3$) in relation to the negative controls without GSH synthesis inhibitor and without activation (–BSO –poly I:C). Significant differences between treatments and Hg^{2+}-free controls of DT40 cells were checked with one-way analysis of variance (*$p < 0.05$, **$p < 0.01$, ***$p < 0.005$). Vertical lines indicate the median effect concentrations (EC50s) of cytotoxicity after 24 h of exposure from WST-1 assay for different treatment groups: red lines for the treatment groups with both BSO and poly I:C (+BSO +Poly I:C), orange lines for the treatment groups with BSO but without poly I:C (+BSO –Poly I:C), and black lines for the treatment groups without BSO because they showed similar EC50s.
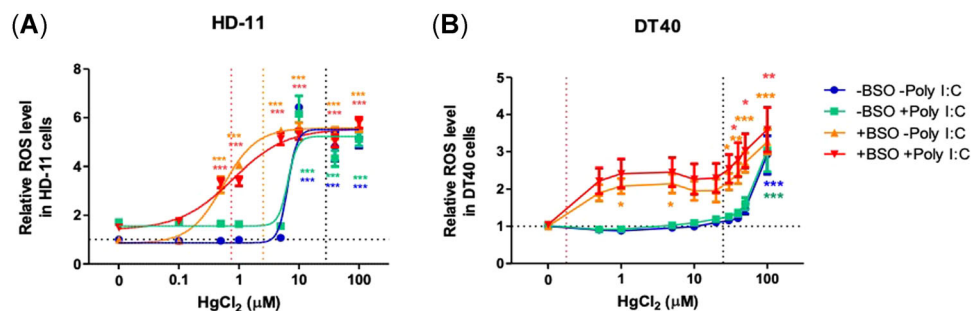
FIGURE 3: Intracellular reactive oxygen species levels after 24-h exposure to mercury $(Hg)^{2+}$ in HD-11 (**A**) and DT40 (**B**) cells with or without glutathione (GSH) synthesis inhibitor (200 μM L-buthionine-sulfoximine [BSO]), and with or without immune stimulator (25 μg/mL poly-inosinic–polycytidylic acid sodium salt [poly I:C]). Results are expressed as a relative ratio (mean ± standard error of the mean, $n = 3$) to the negative controls without GSH synthesis inhibitor and without activation (–BSO –Poly I:C, shown as the horizontal lines). Significant differences between treatments and Hg^{2+}-free controls were checked with one-way analysis of variance (*$p < 0.05$, **$p < 0.01$, ***$p < 0.005$). Vertical lines indicate the median effect concentrations (EC50s) of cytotoxicity after 24-h exposure from the WST-1 assay for different treatment groups: red lines for the treatment groups with both BSO and poly I:C (+BSO +Poly I:C), orange lines for the treatment groups with BSO but without poly I:C (+BSO –Poly I:C), and black lines for the treatment groups without BSO because they showed similar EC50s.

exposure largely depended on poly I:C and also on BSO co-exposure (Figure 4). The poly I:C activation induced nitric oxide production from basal level to more than 10 μM, whereas nonactivated cells hardly generated any nitric oxide. Concentration-dependent inhibition of nitric oxide production was caused by Hg^{2+} exposure in activated cells at noncytotoxic concentrations. Meanwhile, cells became more sensitive with BSO blocking the de novo synthesis of GSH, showing 1 order of magnitude lower EC50 (0.37 μM) than the one without BSO (EC50: 3.85 μM).

Proliferation. As shown in Figure 5, prolonged exposure (48 h) to Hg^{2+} resulted in inhibition of cell proliferation at noncytotoxic concentrations (determined by the 24-h WST-1 assays, shown as vertical lines in Figure 5) in terms of both metabolic activity (WST-1) and DNA synthesis (BrdU) in both cell lines (Figure 5). No significant differences were seen among EC50 values in both cells derived from both assays,
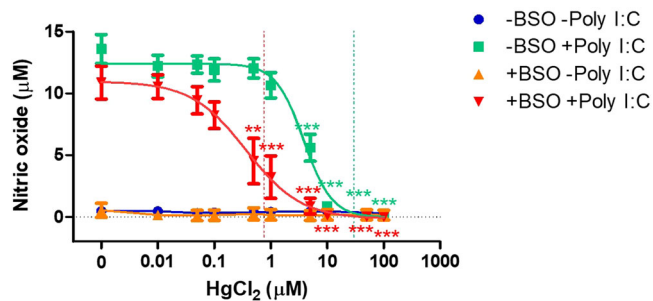
ranging from 2.7 to 6.3 μM (Table 1). In addition, poly I:C treatment significantly stimulated metabolic activity as well as DNA synthesis in DT40 cells (Figure 5C and d, $p < 0.05$), whereas poly I:C significantly inhibited DNA synthesis in HD-11 cells (Figure 5B, $p < 0.05$) without affecting metabolic activity (Figure 5A).

Gene expression. The effect of Hg^{2+} exposure on five immune functional genes and two miRNAs was analyzed. Only miR155 was found to be downregulated in activated DT40 B-lymphocytes. (Figure 6A; detailed results shown in the Supporting Information, Figure S1).

Functional IFN-α and IgM levels. For DT40 B lymphocytes, IgM levels were measured in both culture supernatant and cell lysate. Secreted IgM in culture supernatant did not respond to Hg exposure or poly I:C activation at concentrations below the EC50 for cytotoxicity (data not shown). The IgM detected in cell lysate consisted of the IgM in the cytoplasm and the IgM on the cell membrane functioning as B-cell receptors. The poly I:C stimulated IgM levels in the cell lysate (Figure 6B). Cellular IgM levels in nonactivated DT40 cells significantly decreased after exposed to Hg^{2+}, ranging from 0.01 to 1 μM, followed by a remarkable increase at 10 μM. Because the results were expressed per milligram protein content in the lysate samples, the increase in IgM levels at 10 μM could be due to the low protein content (Supporting Information, Figure S2).

The levels of antiviral IFN-α secreted into the culture supernatant were measured with ELISA assays for both cell lines (Figure 6C and D). An increasing trend of IFN-α with the increasing concentration of Hg^{2+} exposure was noted in both cell lines, especially in DT40 cells. Although significances were only found in high concentrations close to cytotoxic levels, the EC50 values for both nonactivated and activated DT40 cells were as low as 0.5 μM (Table 1). The poly I:C activation did not affect the IFN-α production in either of the cell lines. Compared with DT40 cells, the secretion of IFN-α by HD-11 cells was less responsive to Hg^{2+} exposure, but the initial levels in the non-exposed cells were higher.
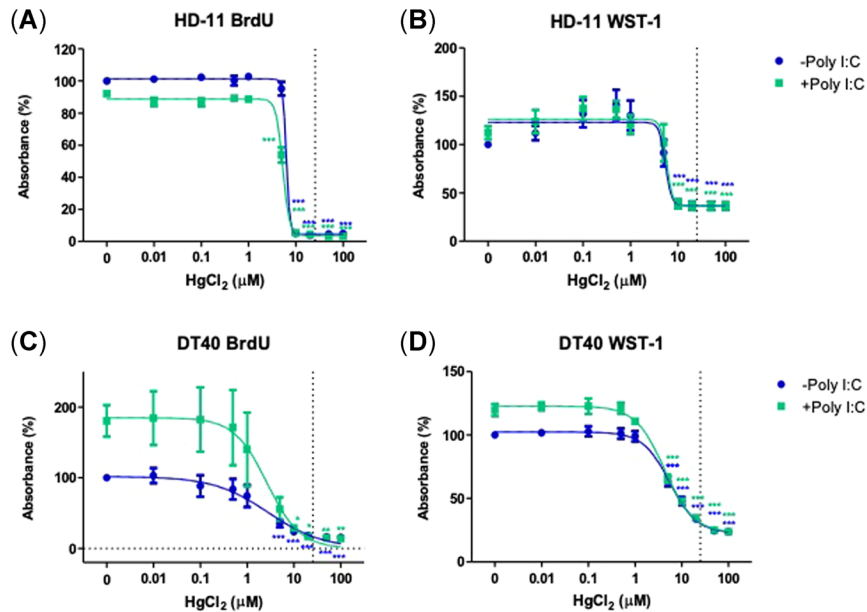

FIGURE 4: Nitric oxide production by activated (with 25 μg/ml poly-inosinic–polycytidylic acid sodium salt [poly I:C]) and nonactivated HD-11 cells with or without glutathione synthesis inhibitor (200 μM L-buthionine-sulfoximine [BSO]) were measured with the Griess assay after 24-h Hg^{2+} exposure. Results are expressed as mean ± standard error of the mean ($n = 3$). Significant differences between treatments and Hg^{2+}-free controls were checked with one-way analysis of variance (**$p < 0.01$, ***$p < 0.005$). Vertical lines indicate the median effect concentrations of cytotoxicity after 24-h exposure from WST-1 assay for different treatments: red line for the treatment group with both BSO and poly I:C (+BSO +Poly I:C), and green line for the treatment group without BSO but with poly I:C (–BSO +Poly I:C).

FIGURE 5: Cell proliferation of HD-11 cells (**A** and **B**) and DT40 cells (**C** and **D**) with and without 25 μg/ml polyinosinic–polycytidylic acid sodium salt activation after 48-h Hg^{2+} exposure. Results are expressed as relative absorbance to negative control in nonactivated groups (mean ± standard error of the mean, $n = 3$), and statistically compared with Hg^{2+}-free negative controls with one-way analysis of variance (*$p < 0.05$, **$p < 0.01$, ***$p < 0.005$). Vertical lines indicate the median effect concentration of cytotoxicity after 24-h exposure from the WST-1 assay for HD-11 cells (**A** and **B**) or DT40 cells (**C** and **D**). BrdU = bromodeoxyuridine; WST-1 = water-soluble tetrazolium-1.

DISCUSSION

General toxicity

Cytotoxicity. The objective of the present study was to investigate in vitro cytotoxic and immune functional effects of Hg^{2+} exposure on two chicken immune cell lines (HD-11 macrophage and DT40 B-lymphocytes as models for specific avian immune cell types), after a viral-like challenge. Similar EC50 values for cell viability (~30 μM) were found for both cell lines after Hg^{2+} exposure for 24 h (Figure 1 and Table 1), which were in the same range of the EC50 values for Hg^{2+} from other in vitro studies using mammalian immune cells (Yamamoto
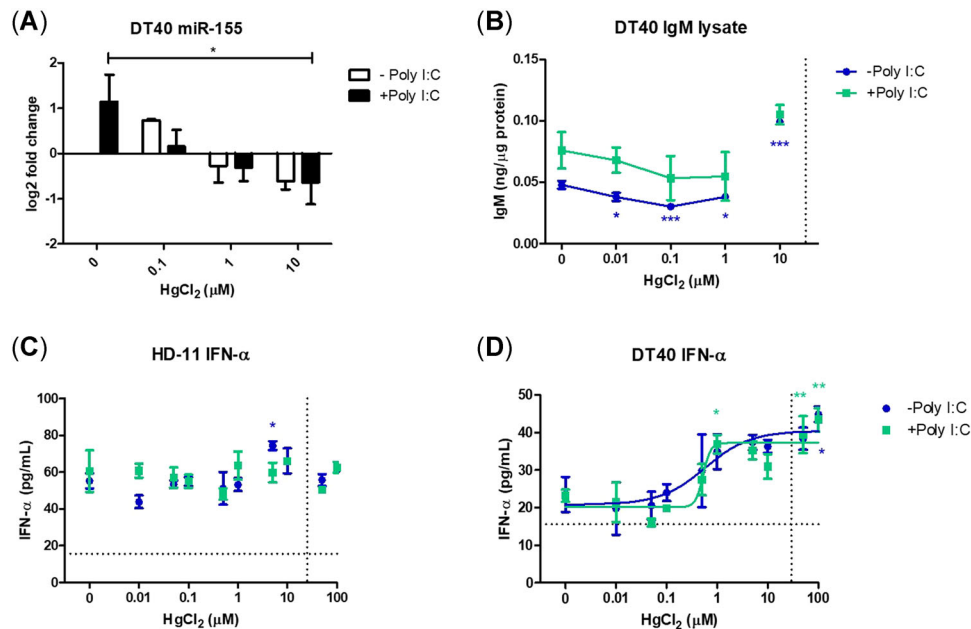

FIGURE 6: Effects of mercury (Hg)$^{2+}$ exposure with and without 25 μg/ml polyinosinic–polycytidylic acid sodium salt activation on expression of miR-155 in DT40 B-lymphocytes (**A**), IgM levels in DT40 cell lysate (**B**), and IFN-α produced by HD-11 (**C**) and DT40 cells (**D**). Results are expressed as mean ± standard error of the mean ($n = 3$), and significant differences between treatments and Hg^{2+}-free controls were checked with one-way analysis of variance (*$p < 0.05$, **$p < 0.01$, ***$p < 0.005$). Vertical lines indicate the median effect concentration values of cytotoxicity after 24-h exposure obtained from the WST-1 assay. Horizontal lines show the detection limits of the IFN-α enzyme-linked immunosorbent assay (15.6 pg/ml). IFN-α = interferon α.

et al., 1998; De Guise et al., 2000; Wataha et al., 2000; Kim & Sharma, 2004; Engin et al., 2017; David et al., 2020). The poly I:C induced cell metabolic activity only in HD-11 macrophage cells but not in DT40 B-cells (Figure 1), but after 48 h of exposure, only DT40 cells showed an increased metabolic activity after poly I:C challenge (Figure 6B and D). These cell- and time-dependent responses might suggest that HD-11 macrophages build a faster response to poly I:C challenge than DT40 B-cells. The poly I:C challenge did not affect the sensitivity of either cell type to Hg^{2+} exposure, because similar EC50 values were obtained. Stimulatory effects on the activity of cells by low Hg^{2+} concentration exposure were seen, especially in HD-11 cells (Figure 1A). Similar hormetic effects have been observed in Hg^{2+}-exposed mammalian cells in vitro, such as bovine leukocytes and a human mammary cell line (De Guise et al., 2000; Schmidt et al., 2004). This may point to cellular stress responses to detoxify the Hg^{2+} and could be important in case of chronic exposure scenarios (Damelin et al., 2000; Calabrese et al., 2007; David et al., 2020).

Compared with other trace metal ions, Hg^{2+} has a relatively high toxicity. For example, the toxicity of lead $(Pb)^{2+}$ was evaluated in the same cell types with much higher EC50 values, namely, 480 µM for HD-11 macrophages and 1700 µM for DT40 lymphocytes (Han et al., 2020). Therefore, although inorganic Hg^{2+} is generally regarded to be less toxic than MeHg, it could still be a trace metal ion of concern.

GSH and ROS. Depletion of GSH and induction of ROS have been identified as major mechanisms of toxicity induced by trace metals with high affinity to the thiol group (Nuran Ercal et al., 2005). In the present study, we included BSO co-exposure, blocking γ-glutamylcysteine synthetase, to investigate the function of de novo synthesis of GSH in the Hg^{2+} exposure experiments. As shown in Figures 1–3, intracellular GSH levels dropped, ROS levels increased, and cell viability decreased in both cell lines after Hg^{2+} exposure without BSO, but when BSO inhibited the de novo GSH synthesis, the EC50 values were much lower. This indicates that depletion of GSH could be one of the major mechanisms of Hg^{2+}-induced toxicity in both cell lines and that the de novo GSH synthesis plays an import role in its detoxification. It is hypothesized that, at noncytotoxic levels, Hg^{2+} depleted endogenous GSH, which at the same time could be compensated for by the de novo production of GSH as a protective response. However, when the Hg^{2+} concentrations became too high, the capacity of the GSH de novo synthesis appeared to be not sufficient, resulting in a depletion of GSH, accumulation of ROS, and loss of cell viability.

Compared with HD-11 cells, DT40 B-cells showed higher sensitivity to Hg^{2+} exposure when BSO was co-exposed in terms of cell viability and intercellular GSH and ROS levels (Figures 1–3). These differences were probably due to the nature of these two types of cells. Macrophages (HD-11) are equipped with a robust and complex antioxidant buffer system, such as lipid mediators and metabolic reprograming, to survive from the high levels of ROS and nitric oxide produced by themselves after activation and consecutive oxidative burst (Brüne et al., 2013; Virág et al., 2019). Meanwhile, DT40 B-cells

apparently rely on de novo GSH synthesis more than HD-11 macrophages, showing a sharp drop in GSH and cell viability already at the lowest Hg^{2+} exposure concentration (0.5 µM) after co-exposure with BSO. However, without BSO, HD-11 macrophages were more sensitive to Hg^{2+} exposure regarding GSH levels (Figure 2; with a EC50 at 15 µM) than DT40 B-cells (EC50 values between 50 and 100 µM). Decreased GSH levels in DT40 cells were only seen above cytotoxic Hg^{2+} concentrations, suggesting that there might be other mechanisms inducing cell viability besides GSH depletion.

These cell-specific effects demonstrated that under normal circumstances (without BSO) HD-11 macrophages are probably more vulnerable to Hg^{2+}-induced GSH depletion and ROS induction resulting in decreased cell viability with lower EC50 values than DT40 B-lymphocytes. Also, according to our results with BSO blocking the de novo GSH synthesis, macrophages are thought to be protected by a more complex antioxidative protective system against ROS, which likely includes other components than GSH, such as metabolic reprogramming bioactive and lipid mediators (Virág et al., 2019). These additional protective mechanisms are still effective after BSO exposure. However, the DT40 cell relies largely on GSH as an antioxidant.

Immune functional endpoints

Nitric oxide. In addition to cytotoxic effects, modulatory effects of Hg^{2+} on some functional endpoints were also detected in both cell lines at noncytotoxic concentrations. For instance, nitric oxide production was found to be strongly inhibited by Hg^{2+} in activated HD-11 macrophages (Figure 4), as also reported in murine macrophages (Tian & Lawrence, 1996; Kim et al., 2002; Batista-Duharte et al., 2018). Downregulation of inducible nitric oxide synthase in cells of the J774A.1 murine macrophage cell line by Hg^{2+} was demonstrated in both gene expression profiles as well as protein levels (Kim et al., 2002). However, increased nitric oxide levels were found in activated macrophage cell lines after noncytotoxic levels of cadmium $(Cd)^{2+}$ and Pb^{2+} exposure (García-Mendoza et al., 2019; Han et al., 2020), suggesting possible deviating mechanisms among divalent trace metal irons. Once the GSH synthesis was blocked by BSO, less nitric oxide was produced by activated HD-11 cells exposed to Hg^{2+} between 0.5 and 5 µM (Figure 4). This could be related to the decreased cell viability (Figure 1A).

In addition, oxidized glutathione (in our case triggered by the treatment with BSO in activated cells) may induce S-glutathionylation of the nitric oxide synthase enzyme (NOS) via exchanging thiol–disulphide, leading to uncoupling of biochemically active NOS dimers and a switch from the production of nitric oxide to other types of ROS (Chen et al., 2010; Dulce et al., 2011). This might be explained by the fact that the capacity of the protective cellular antioxidant determines how much nitric oxide macrophage cells can produce, to prevent cells from injuring themselves. Nitric oxide is involved in more immune functions than direct antimicrobial activities, such as regulation of cytokine production and lymphocytes differentiation (MacMicking et al., 1997; Bogdan, 2001; Tripathi et al., 2007). Hence, inhibited nitric oxide production after
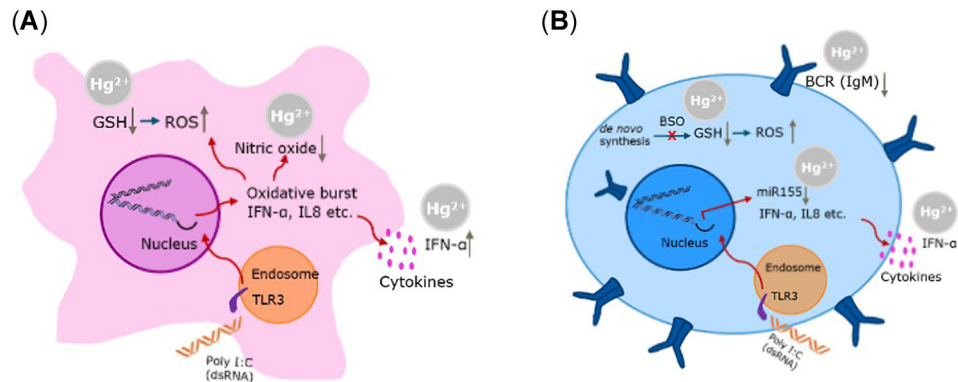
FIGURE 7: Effects of mercury (Hg)$^{2+}$ on the immune functions found in HD-11 macrophage (**A**) and DT40 B-lymphocyte (**B**). GSH = glutathione; ROS = reactive oxygen species; IFN-α = interferon-α; IL8 = interleukin 8; TLR3 = toll-like receptor 3; poly I:C = polyinosinic acid-polycytidylic acid; dsRNA = double-stranded RNA; BSO = buthionine sulphoximine; miR-155 = microRNA 155.

Hg^{2+} exposure in activated macrophages can cause an impaired antimicrobial response as well as disturbed immune signaling and might lead to higher risks of infections in vivo.

Proliferation. Proliferation of cells was supressed by Hg^{2+} exposure in both cell lines regardless of activation, affecting both DNA replication (Figure 5A and C) and metabolic activity (Figure 5B and D). The DT40 cells were slightly more sensitive to Hg^{2+} than HD-11 macrophages, with approximately 2-fold lower EC50 in BrdU assays (Table 1). Decreased immune cell proliferation due to Hg^{2+} exposure was also indicated in mice ex vivo, depending on age and organ (Silva et al., 2005). On the other hand, some studies have suggested stimulatory effects of low-level Hg^{2+} exposure on murine lymphocyte proliferation (Pelletier et al., 1985; Jiang & Möller, 1996; Pollard & Landberg, 2001). Although hormesis was not found in the proliferation assays after 48 h of exposure (Figure 5), it was seen in the WST-1 assays after 24 h of exposure (Figure 1). This might suggest that the effect on increased cell metabolic activities is a rather acute response. Interestingly, after poly I:C activation, HD-11 cells tended to slightly decrease DNA synthesis, potentially to maintain cell homeostasis, whereas DT40 cells showed enhancement in both DNA synthesis and cell activity. In addition, similar EC50 values between unstimulated and stimulated cells suggest that poly I:C challenge did not affect the sensitivity of cells to Hg^{2+} exposure (Table 1). Our results indicate that Hg^{2+} exposure may cause a deficiency in functional immune cells and may disturb the immune cell composition in avian species in vivo.

Gene expression and immune protein. Gene expression and protein levels were measured as major immune parameters in the present study. The poly I:C was reported to be recognized by TLR3, triggering several pathways such as nuclear factor κB (NF-κB) and interferon receptor factors (IRFs) pathways, resulting in generation of a spectrum of cytokines including proinflammatory cytokines (e.g., IL-8 and IL-18) via the NF-κB pathway and antiviral type I IFNs (IFN-α and -β) via IRFs pathways (Alexopoulou et al., 2001; Moynagh, 2005; Sen & Sarkar, 2005; Kawasaki & Kawai, 2014). Our results demonstrated a significant increase in IFN-α levels due to Hg^{2+} exposure in both cell lines, especially DT40 cells (Figure 6C and D), similar to what was observed in Pb^{2+}-exposed HD-11 and DT40 cells (Han et al., 2020). Although the expression of type I IFNs was documented to be lifted in HD-11 cells after 2 h of incubation with poly I:C (Peroval et al., 2013), different IFN-α levels after poly I:C activation were not found in the qPCR or the ELISA assays after 24 h of exposure in the present study. The prolonged stimulation time could have resulted in the degradation of the induced IFNs by poly I:C. In addition, because both HD-11 and DT40 are immortal cell lines transformed with virus (MC29 virus for HD-11 cells and avian leukosis virus for DT40 cells; Beug et al., 1979; Bezzubova & Buerstedde, 1994), they might have to some extent lost their capacity for type I IFN production after viral-like challenge with poly I:C.

The HD-11 cells were found not to produce more type I IFN after infection with the highly pathogenic avian influenza virus H5N1, whereas both ex vivo (in primary chicken splenocytes) and in vivo (in chicken) studies showed significantly increased type I IFN production after infection with the same virus (Liniger et al., 2012). This difference could be due to the presence of specialized type I IFN-producing cells in primary splenocytes and in vivo, and might suggest a deficiency in type I IFN production in HD-11 cells after viral challenge. Type I IFNs secreted by immune cells can pass the signal to the neighboring cells, which will develop an antiviral state to defend themselves against the infection. However, excessive type I IFNs may promote autoimmunity in vivo (Baccala et al., 2007). Therefore, the type I IFN induced by Hg^{2+} exposure might potentially result in a disorder of immunity.

Apart from cytokines, another group of crucial immune mediators is the miRNAs, which can regulate cellular activities posttranscriptionally by inhibiting translation and destabilizing mRNA (Bushati & Cohen, 2007). As a multifunctional miRNA, miR-155 is involved in regulation of lymphocyte proliferation and differentiation, macrophage polarization, antibody production, and other functions (Alivernini et al., 2018). Our results indicated that miR-155 was down-regulated by 10 μM Hg^{2+} in activated DT40 B-lymphocytes (Figure 6A). Decreased miR-155 levels caused impaired B-cell proliferation in mouse models (Rodriguez

2822

Environmental Toxicology and Chemistry, 2021;40:2813–2824—B. Han et al.

et al., 2007; Babar et al., 2012), which is in line with our results (Figure 5). In addition, cellular IgM content was found to be significantly decreased by noncytotoxic Hg^{2+} exposure in the cell lysate of nonactivated DT40 lymphocytes, but not in activated cells (Figure 6B). The IgM in the cell lysate referred mainly to the IgM on the cell membrane acting as B-cell receptors (BCRs), which can recognize antigens and initiate humoral immunity (Friess et al., 2018). Therefore, Hg^{2+} affected B-cell functions probably by suppressing miR-155 expression after activation and decreasing membrane BCRs on the cell membrane without activation. This might result in a weakened pathogen defence and higher risk of infection in avian species.

CONCLUSIONS

In summary, the results of the present study revealed that Hg^{2+} had concentration-dependent toxic effects on both chicken macrophage (HD-11) and B-lymphocyte (DT40) cells and affected their immune functions (Figure 7). De novo GSH production played a vital role in protecting the cells from Hg^{2+}-related GSH depletion and ROS induction, and meanwhile could influence the immune function of activated HD-11 macrophages with respect to nitric oxide production. In addition, antiviral IFN-α levels were elevated by Hg^{2+} in both cell types. In B-lymphocytes, Hg^{2+} mainly downregulated the expression of miR155 after activation and decreased the cellular IgM levels, which probably act as BCRs, without activation. Based on the present study, it is likely that Hg^{2+} may disturb the homeostasis of the avian immune system, potentially resulting in an inadequate immune response after viral infections that might cause a higher risk of infection for individuals and even prevalence of diseases in the group. Although we only employed two in vitro cell models (macrophages and B-lymphocytes) without considering the other parts of the immune system and interactions between immune cells, our results provide a starting point for future studies on molecular mechanisms, systematic immune responses, and effects of long-term exposure to immune-toxic trace metals in avian species after viral challenges.

REFERENCES

Ackerman, J. T., Eagles-Smith, C. A., Herzog, M. P., Hartman, C. A., Peterson, S. H., Evers, D. C., Jackson, A. K., Elliott, J. E., Vander Pol, S. S., & Bryan, C. E. (2016). Avian mercury exposure and toxicological risk across western North America: A synthesis. *Science of the Total Environment*, *568*, 749–769. https://doi.org/10.1016/j.scitotenv.2016.03.071

Alexopoulou, L., Holt, A. C., Medzhitov, R., & Flavell, R. A. (2001). Recognition of double-stranded RNA and activation of NF-κB by Toll-like receptor 3. *Nature*, *413*(6857), 732–738. https://doi.org/10.1038/35099560

Alivernini, S., Gremese, E., McSharry, C., Tolusso, B., Ferraccioli, G., McInnes, I. B., & Kurowska-Stolarska, M. (2018). MicroRNA-155-at the critical interface of innate and adaptive immunity in arthritis. *Frontiers in immunology*, *8*(05 January). https://doi.org/10.3389/fimmu.2017.01932

Babar, I. A., Cheng, C. J., Booth, C. J., Liang, X., Weidhaas, J. B., Saltzman, W. M., & Slack, F. J. (2012). Nanoparticle-based therapy in an in vivo microRNA-155 (miR-155)-dependent mouse model of lymphoma. *Proceedings of the National Academy of Sciences USA*, *109*(26), E1695–E1704. https://doi.org/10.1073/pnas.1201516109

Baccala, R., Hoebe, K., Kono, D. H., Beutle, B., & Theofilopoulos, A. N. (2007). TLR-dependent and TLR-independent pathways of type I interferon induction in systemic autoimmunity. *Nature Medicine*, *13*(5), 543–551. https://doi.org/10.1038/nm1590

Batista-Duharte, A., Téllez-Martínez, D., Jellmayer, J. A., Fuentes, D. L. P., Polesi, M. C., Baviera, A. M., & Carlos, I. Z. (2018). Repeated exposition to mercury (II) chloride enhances susceptibility to s. schenckii sensu stricto infection in mice. *Journal of Fungi*, *4*(2). https://doi.org/10.3390/jof4020064

Beckers, F., & Rinklebe, J. (2017). Cycling of mercury in the environment: Sources, fate, and human health implications: A review. *Critical Reviews Environmental Science and Technology*, *47*(9), 693–794. https://doi.org/10.1080/10643389.2017.1326277

Beug, H., von Kirchbach, A., Döderlein, G., Conscience, J. F., & Graf, T. (1979). Chicken hematopoietic cells transformed by seven strains of defective avian leukemia viruses display three distinct phenotypes of differentiation. *Cell*, *18*(2), 375–390. https://doi.org/10.1016/0092-8674(79)90057-6

Bezzubova, O. Y., & Buerstedde, J. M. (1994). Gene conversion in the chicken immunoglobulin locus: A paradigm of homologous recombination in higher eukaryotes. *Experientia*, *50*(3), 270–276. https://doi.org/10.1007/BF01924010

Bogdan, C. (2001). Nitric oxide and the immune response. *Nature Immunology*, *2*(10), 907–916. https://doi.org/10.1038/ni1001-907

Brüne, B., Dehne, N., Grossmann, N., Jung, M., Namgaladze, D., Schmid, T., Von Knethen, A., & Weigert, A. (2013). Redox control of inflammation in macrophages. *Antioxidants and Redox Signaling*, *19*(6), 595–637. https://doi.org/10.1089/ars.2012.4785

Bushati, N., & Cohen, S. M. (2007). MicroRNA functions. *Annual Review of Cell Development Biology*, *23*, 175–205. https://doi.org/10.1146/annurev.cellbio.23.090506.123406

Calabrese, E. J., Bachmann, K. A., Bailer, A. J., Bolger, P. M., Borak, J., Cai, L., Cedergreen, N., Cherian, M. G., Chiueh, C. C., Clarkson, T. W., Cook, R. R., Diamond, D. M., Doolittle, D. J., Dorato, M. A., Duke, S. O., Feinendegen, L., Gardner, D. E., Hart, R. W., Hastings, K. L., & Mattson, M. P. (2007). Biological stress response terminology: Integrating the concepts of adaptive response and preconditioning stress within a hormetic dose-response framework. *Toxicology and Applied Pharmacology*, *222*(1), 122–128. https://doi.org/10.1016/j.taap.2007.02.015

Chen, C. A., Wang, T. Y., Varadharaj, S., Reyes, L. A., Hemann, C., Talukder, M. A. H., Chen, Y. R., Druhan, L. J., & Zweier, J. L. (2010). S-glutathionylation uncouples eNOS and regulates its cellular and vascular function. *Nature*, *468*(7327), 1115–1120. https://doi.org/10.1038/nature09599

Damelin, L. H., Vokes, S., Whitcutt, J. M., Damelin, S. B., & Alexander, J. J. (2000). Hormesis: A stress response in cells exposed to low levels of heavy metals. *Human & Experimental Toxicology*, *19*(7), 420–430. https://doi.org/10.1191/096032700678816133

Das, K., Siebert, U., Gillet, A., Dupont, A., Di-Poï, C., Fonfara, S., Mazzucchelli, G., De Pauw, E., & De Pauw-Gillet, M. C. (2008). Mercury immune toxicity in harbour seals: Links to in vitro toxicity. *Environmental Health: A Global Access Science Source*. https://doi.org/10.1186/1476-069X-7-52

David, J., Muniroh, M., Nandakumar, A., Tsuji, M., Koriyama, C., & Yamamoto, M. (2020). Inorganic mercury-induced mip-2 expression is suppresseby n-acetyl-l-cysteine in raw264.7 macrophages. *Biomedical Reports*, *12*(2), 39–45. https://doi.org/10.3892/br.2019.1263

De Guise, S., Bernier, J., Lapierre, P., Dufresne, M. M., Dubreuil, P., & Fournier, M. (2000). Immune function of bovine leukocytes after in vitro exposure to selected heavy metals. *American Journal of Veterinary Research*, 61(3), 339–344. https://doi.org/10.2460/ajvr.2000.61.339

Dorea, J. G., & Donangelo, C. M. (2006). Early (in uterus and infant) exposure to mercury and lead. *Clinical Nutrition*, 25(3), 369–376. https://doi.org/10.1016/j.clnu.2005.10.007

Dörner, T., & Radbruch, A. (2007). Antibodies and B cell memory in viral immunity. *Immunity*, 27(3), 384–392. https://doi.org/10.1016/j.immuni.2007.09.002

Dulce, R. A., Schulman, I. H., & Hare, J. M. (2011). S-glutathionylation: A redox-sensitive switch participating in nitroso-redox balance. *Circulation Research*, 108(5), 531–533. https://doi.org/10.1161/RES.0b013e3182147d74

Engin, A. B., Engin, E. D., Golokhvast, K., Spandidos, D. A., & Tsatsakis, A. M. (2017). Glutamate-mediated effects of caffeine and interferon-γ on mercury-induced toxicity. *International Journal of Molecular Medicine*, 39(5), 1215–1223. https://doi.org/10.3892/ijmm.2017.2937

Finkelstein, M. E., Grasman, K. A., Croll, D. A., Tershy, B. R., Keitt, B. S., Jarman, W. M., & Smith, D. R. (2007). Contaminant-associated alteration of immune function in black-footed albatross (Phoebastria nigripes), a North Pacific predator. *Environmental and Toxicological. Chemistry*, 26(9), 1896–1903. https://doi.org/10.1897/06-505R.1

Friess, M. D., Pluhackova, K., & Böckmann, R. A. (2018). Structural model of the mIgM B-cell receptor transmembrane domain from self-association molecular dynamics simulations. *Frontiers in immunology*, 9, 2947. https://doi.org/10.3389/fimmu.2018.02947

García-Mendoza, D., Han, B., van den Berg, H. J. H. J., & van den Brink, N. W. (2019). Cell-specific immune-modulation of cadmium on murine macrophages and mast cell lines in vitro. *Journal of Applied Toxicology*, 39(7), https://doi.org/10.1002/jat.3788

Gottwein, E., Mukherjee, N., Sachse, C., Frenzel, C., Majoros, W. H., Chi, J. T. A., Braich, R., Manoharan, M., Soutschek, J., Ohler, U., & Cullen, B. R. (2007). A viral microRNA functions as an orthologue of cellular miR-155. *Nature*, 450(7172), 1096–1099. https://doi.org/10.1038/nature05992

Guzzi, G. P., & La Porta, C. A. M. (2008). Molecular mechanisms triggered by mercury. *Toxicology*, 244(1), 1–12. https://doi.org/10.1016/j.tox.2007.11.002

Han, B., García-Mendoza, D., van den Berg, H., & van den Brink, N. W. (2020). Modulatory effects of Pb2+ on virally challenged chicken macrophage (HD-11) and B-lymphocyte (DT40) cell lines in vitro. *Environmental and Toxicological Chemistry*, 39(5), 1060–1070. https://doi.org/10.1002/etc.4702

Hawley, D. M., Hallinger, K. K., & Cristol, D. A. (2009). Compromised immune competence in free-living tree swallows exposed to mercury. *Ecotoxicology*, 18(5), 499–503. https://doi.org/10.1007/s10646-009-0307-4

He, H., Genovese, K. J., Nisbet, D. J., & Kogut, M. H. (2007). Synergy of CpG oligodeoxynucleotide and double-stranded RNA (poly I:C) on nitric oxide induction in chicken peripheral blood monocytes. *Molecular Immunology*, 44(12), 3234–3242. https://doi.org/10.1016/j.molimm.2007.01.034

Hossain, K. F. B., Rahman, M. M., Sikder, M. T., Hosokawa, T., Saito, T., & Kurasaki, M. (2021). Selenium modulates inorganic mercury induced cytotoxicity and intrinsic apoptosis in PC12 cells. *Ecotoxicology and Environmental Safety*, 207, 111262. https://doi.org/10.1016/j.ecoenv.2020.111262

Hultberg, B., Andersson, A., & Isaksson, A. (2001). Interaction of metals and thiols in cell damage and glutathione distribution: Potentiation of mercury toxicity by dithiothreitol. *Toxicology*, 156(2–3), 93–100. https://doi.org/10.1016/S0300-483X(00)00331-0

Jiang, Y., & Möller, G. (1996). In vitro effects of HgCl2 on murine lymphocytes. II. Selective activation of T cells expressing certain V(β) TCR. *International Immunology*, 8(11), 1729–1736. https://doi.org/10.1093/intimm/8.11.1729

Kaiser, P., & Stäheli, P. (2013). Avian cytokines and chemokines. In K. A. Schat, B. Kaspers & P. Kaiser (Eds.), *Avian immunology* (4th ed., pp. 189–204). Elsevier

Kawasaki, T., & Kawai, T. (2014). Toll-like receptor signaling pathways. *Frontiers in Immunology*, 5(September). https://doi.org/10.3389/fimmu.2014.00461

Keestra, A. M., & van Putten, J. P. M. (2008). Unique properties of the chicken TLR4/MD-2 complex: Selective lipopolysaccharide activation of the MyD88-dependent pathway. *Journal of Immunology*, 181(6), 4354–4362. https://doi.org/10.4049/jimmunol.181.6.4354

Kim, S. H., Johnson, V. J., & Sharma, R. P. (2002). Mercury inhibits nitric oxide production but activates proinflammatory cytokine expression in murine macrophage: Differential modulation of NF-κB and p38 MAPK signaling pathways. *Nitric Oxide Biology and Chemistry*, 7(1), 67–74. https://doi.org/10.1016/S1089-8603(02)00008-3

Kim, S. H., & Sharma, R. P. (2004). Mercury-induced apoptosis and necrosis in murine macrophages: Role of calcium-induced reactive oxygen species and p38 mitogen-activated protein kinase signaling. *Toxicological and Applied Pharmacology*, 196(1), 47–57. https://doi.org/10.1016/j.taap.2003.11.020

Kumar, M., Sahu, S. K., Kumar, R., Subuddhi, A., Maji, R. K., Jana, K., Gupta, P., Raffetseder, J., Lerm, M., Ghosh, Z., van Loo, G., Bevaert, R., Gupta, U. D., Kundu, M., & Basu, J. (2015). MicroRNA let-7 modulates the immune response to mycobacterium tuberculosis infection via control of A20, an inhibitor of the NF-κB pathway. *Cell Host & Microbe*, 17(3), 345–356. https://doi.org/10.1016/j.chom.2015.01.007

Lehmann, I., Sack, U., & Lehmann, J. (2011). Metal ions affecting the immune system. In H. Sigel, A. Sigel & R. K. O. Sigel (Eds.). *Metal ions in toxicology: Effects, interactions, interdependencies.* Vol. 8. (pp. 157–186). De Gruyter.

Levin, M., Jasperse, L., Desforges, J. P., O'Hara, T., Rea, L., Castellini, J. M., Maniscalco, J. M., Fadely, B., & Keogh, M. (2020). Methyl mercury (MeHg) in vitro exposure alters mitogen-induced lymphocyte proliferation and cytokine expression in Steller sea lion (Eumetopias jubatus) pups. *Science of the Total Environment*, 725, 138308. https://doi.org/10.1016/j.scitotenv.2020.138308

Liniger, M., Moulin, H. R., Sakoda, Y., Ruggli, N., & Summerfield, A. (2012). Highly pathogenic avian influenza virus H5N1 controls type I IFN induction in chicken macrophage HD-11 cells: A polygenic trait that involves NS1 and the polymerase complex. *Virology Journal*, 9, 7. https://doi.org/10.1186/1743-422x-9-7

Loftenius, A., Ekstrand, J., & Möller, K. (1997). In vitro effects of mercuric chloride (HgCl2) on human mononuclear cells. *Clinical and Expimental Immunology*, 110(3), 418–422. https://doi.org/10.1046/j.1365-2249.1997.4531470.x

Lu, L. F., & Liston, A. (2009). MicroRNA in the immune system, microRNA as an immune system. *Immunology*, 127(3), 291–298. https://doi.org/10.1111/j.1365-2567.2009.03092.x

Ma, Y., Liang, Y., Wang, N., Cui, L., Chen, Z., Wu, H., Zhu, C., Wang, Z., Liu, S., & Li, H. (2019). Avian flavivirus infection of monocytes/macrophages by extensive subversion of host antiviral innate immune responses. *Journal of Virology*, 93(22), 978–997. https://doi.org/10.1128/JVI.00978-19

MacMicking, J., Xie, Q. W., & Nathan, C. (1997). Nitric oxide and macrophage function. *Annual Review of Immunology*, 15, 323–350. https://doi.org/10.1146/annurev.immunol.15.1.323

Mann, R. M., Vijver, M. G., & Peijnenburg, W. J. G. M. (2011). Metals and metalloids in terrestrial systems: Bioaccumulation, biomagnification and subsequent adverse effects. In F. Sánchez-Bayo, P. J. van den Brink, & R. M. Mann (Eds.). *Ecological impacts of toxic chemicals* (pp. 43–62). Bentham Science Publishers.

Matsumoto, M., & Tsukasa, S. (2008). TLR3: Interferon induction by double-stranded RNA including poly(I:C). *Advances in Drug Delivery Review*, 60(7), 805–812. https://doi.org/10.1016/j.addr.2007.11.005

Mogensen, T. H. (2009). Pathogen recognition and inflammatory signaling in innate immune defenses. *Clinical Microbiology Review*, 22(2), 240–273. https://doi.org/10.1128/CMR.00046-08

Moynagh, P. N. (2005). TLR signalling and activation of IRFs: Revisiting old friends from the NF-κB pathway. *Trends in Immunology*, 26(9), 469–476. https://doi.org/10.1016/j.it.2005.06.009

Nuran Ercal, B. S. P., Hande Gurer-Orhan, B. S. P., & Nukhet Aykin-Burns, B. S. P. (2005). Toxic metals and oxidative stress Part I: Mechanisms involved in metal induced oxidative damage. *Current Topics in Medicine and Chemistry*, 1(6), 529–539. https://doi.org/10.2174/1568026013394831

Pelletier, L., Pasquier, R., Hirsch, F., Sapin, C., & Druet, P. (1985). In vivo self-reactivity of mononuclear cells to T cells and macrophages exposed to HgCl2. *European Journal of Immunology*, 15(5), 460–465. https://doi.org/10.1002/eji.1830150509

Peroval, M. Y., Boyd, A. C., Young, J. R., & Smith, A. L. (2013). A critical role for MAPK signalling pathways in the transcriptional regulation of Toll like

receptors. *PLoS One*, 8(2), e51243. https://doi.org/10.1371/journal.pone.0051243

Pollard, K. M., & Landberg, G. P. (2001). The in vitro proliferation of murine lymphocytes to mercuric chloride is restricted to mature T cells and is interleukin 1 dependent. *International Immunopharmacology*, 1(3), 581–593. https://doi.org/10.1016/S1567-5769(00)00034-5

Quan, R., Zhu, S., Wei, L., Wang, J., Yan, X., Li, Z., & Liu, J. (2017). Transcriptional profiles in bursal B-lymphoid DT40 cells infected with very virulent infectious bursal disease virus. *Virology Journal*, 14(1), 7. https://doi.org/10.1186/s12985-016-0668-2

Rodriguez, A., Vigorito, E., Clare, S., Warren, M. V., Couttet, P., Soond, D. R., Van Dongen, S., Grocock, R. J., Das, P. P., Miska, E. A., Vetrie, D., Okkenhaug, K., Anright, A. J., Dougan, G., Turner, M., & Bradley, A. (2007). Requirement of bic/microRNA-155 for normal immune function. *Science*, 316(5824), 608–611. https://doi.org/10.1126/science.1139253

Rosenkranz, A. R., Schmaldienst, S., Stuhlmeier, K. M., Chen, W., Knapp, W., & Zlabinger, G. J. (1992). A microplate assay for the detection of oxidative products using 2′,7′-dichlorofluorescin-diacetate. *Journal of Immunology Methods*, 156(1), 39–45. https://doi.org/10.1016/0022-1759(92)90008-H

Schlüter, K. (2000). Review: Evaporation of mercury from soils. An integration and synthesis of current knowledge. *Environmental Geology*, 39(3–4), 249–271. https://doi.org/10.1007/s002540050005

Schmidt, C. M., Cheng, C. N., Marino, A., Konsoula, R., & Barile, F. (2004). Hormesis effect of trace metals on cultured normal and immortal human mammary cells. *Toxicology and Health*, 20(5), 57–68. https://doi.org/10.1191/0748233704th192oa

Schmittgen, T. D., & Livak, K. J. (2008). Analyzing real-time PCR data by the comparative CT method. *Nature Protocols*, 3(6), 1101–1108. https://doi.org/10.1038/nprot.2008.73

Sen, G. C., & Sarkar, S. N. (2005). Transcriptional signaling by double-stranded RNA: Role of TLR3. *Cytokine and Growth Factor Review*, 16(1), 1–14. https://doi.org/10.1016/j.cytogfr.2005.01.006

Silva, I. A., Graber, J., Nyland, J. F., & Silbergeld, E. K. (2005). In vitro HgCl2 exposure of immune cells at different stages of maturation: Effects on phenotype and function. *Environmental Research*, 98(3), 341–348. https://doi.org/10.1016/j.envres.2005.01.006

Staedel, C., & Darfeuille, F. (2013). MicroRNAs and bacterial infection. *Cell Microbiology*, 15(9), 1496–1507. https://doi.org/10.1111/cmi.12159

Sun, J., Zhang, X., Broderick, M., & Fein, H. (2003). Measurement of nitric oxide production in biological systems by using Griess reaction assay. *Sensors*, 3(8), 276–284. https://doi.org/10.3390/s30800276

Thaxton, P., & Parkhurst, C. R. (1973). Toxicity of mercury to young chickens. 3. Changes in immunological responsiveness. *Poultry Science*, 52(2), 761–764. https://doi.org/10.3382/ps.0520761

Tian, L., & Lawrence, D. A. (1996). Metal-induced modulation of nitric oxide production in vitro by murine macrophages: Lead, nickel, and cobalt utilize different mechanisms. *Toxicology and Applied Pharmacology*, 141(2), 540–547. https://doi.org/10.1006/taap.1996.0320

Tripathi, P., Tripathi, P., Kashyap, L., & Singh, V. (2007). The role of nitric oxide in inflammatory reactions. *FEMS Immunology and Medical Microbiology*, 51(3), 443–452. https://doi.org/10.1111/j.1574-695X.2007.00329.x

Virág, L., Jaén, R. I., Regdon, Z., Boscá, L., & Prieto, P. (2019). Self-defense of macrophages against oxidative injury: Fighting for their own survival. *Redox Biology*, 26, 101261. https://doi.org/10.1016/j.redox.2019.101261

Wataha, J. C., Lockwood, P. E., & Schedle, A. (2000). Effect of silver, copper, mercury, and nickel ions on cellular proliferation during extended, low-dose exposures. *Journal of Biomedical Materials Research*, 52(2), 360–364. https://doi.org/10.1002/1097-4636(200011)52:2<360::AID-JBM16>3.0.CO;2-B

Whitney, M. C., & Cristol, D. A. (2018). Impacts of sublethal mercury exposure on birds: A detailed review (pp. 113–163). In P. de Voogt (Ed.). *Reviews of environmental contamination and toxicology*. Vol. 244. Springer.

Wolfe, M. F., Schwarzbach, S., & Sulaiman, R. A. (1998). Effects of mercury on wildlife: A comprehensive review. *Environmental and Toxicological Chemistry*, 17(2), 146–160. https://doi.org/10.1002/etc.5620170203

Yamamoto, A., Honma, R., & Sumita, M. (1998). Cytotoxicity evaluation of 43 metal salts using murine fibroblasts and osteoblastic cells. *Journal of Biomedical Materials Research*, 39(2), 331–340. https://doi.org/10.1002/(SICI)1097-4636(199802)39:2<331::AID-JBM22>3.0.CO;2-E

Yang, L., Zhang, Y., Wang, F., Luo, Z., Guo, S., & Strähle, U. (2020). Toxicity of mercury: Molecular evidence. *Chemosphere*, 245, 125586. https://doi.org/10.1016/j.chemosphere.2019.125586

Zou, H., Su, R., Ruan, J., Shao, H., Qian, K., Ye, J., Yao, Y., Nair, V., & Qin, A. (2017). Double-stranded RNA induces chicken T-cell lymphoma apoptosis by TRIF and NF-κB. *Science Reports*, 7(1), 7547. https://doi.org/10.1038/s41598-017-07919-w